



AIT Series

Trends in earth observation

Volume 1

Earth observation advancements in a changing world

Edited by Chirici G. and Gianinetto M.



Earth observation advancements in a changing world

Edited by

Gherardo Chirici and Marco Gianinetto

AIT Series: Trends in earth observation



Volume 1 - Published in July 2019
Edited by Gherardo Chirici and Marco Gianinetto
Published on behalf of the Associazione Italiana di Telerilevamento (AIT)
Via Lucca 50
50142 Firenze, Italy

ISSN 2612-7148
ISBN 978-88-944687-1-7
DOI: 10.978.88944687/17

All contributions published in the Volume “Earth observation advancements in a changing world” were subject to blind peer review from independent reviewers.

Publication Ethics and Publication Malpractice Statement
Editors, Reviewers and Authors agreed with Publication Ethics and Publication Malpractice Statement

© 2019 by the authors; licensee Italian Society of Remote Sensing (AIT).
This Volume is an open access volume distributed under the terms and conditions of the Creative Commons Attribution license (<http://creativecommons.org/licenses/by/4.0/>).



Contents

Introduction	vii
Remote sensing advancements to support modern agriculture practices	1
1. Using hyperspectral data to differentiate shade coffee varieties with and without rust and other canopy species	2
<i>N. Corona-Romero, J.M. Madrigal Gómez, M. González-Stefanoni</i>	
2. Waiting for “institutional” monitoring services of rice crops by remote sensing: is cadastral parcel the proper reference geometry?	6
<i>G. Corvino, A. Lessio, E. Borgogno Mondino</i>	
3. A plot sampling strategy for estimating the area of olive tree crops and olive tree abundance in a mediterranean environment	11
<i>M. Grotti, N. Puletti, F. Chianucci, W. Mattioli, A. Floris, F. Clementel, C. Torresan, M. Marchi, A. Gentile, M. Pisante, A. Marcelli, P. Corona</i>	
4. Phenology and yield assessment in maize seed crops using sentinel 2 vis’ time series	15
<i>M. Croci, F. Calegari, P. Morandi, S. Amaducci, M. Vincini</i>	
5. Use of Sentinel-2 images for water needs monitoring: application on an industrial tomato crop in central Italy	19
<i>B. Rapi, L. Angeli, P. Battista, M. Chiesi, R. Magno, A. Materassi, M. Pieri, M. Romani, F. Sabatini, F. Maselli</i>	
6. MODIS EVI time series to assess new oil palm plantation dynamics in Borneo	23
<i>S. De Petris, P. Boccardo, E. Borgogno-Mondino</i>	
7. Remote sensing characterization of crop vulnerability to flood	28
<i>T. Pacetti, E. Caporali, M.C. Rulli</i>	
Earth observation for monitoring forest resources and environmental processes	32
8. Tree species classification with Sentinel-2 data in european part of Russia	33
<i>E.A. Kurbanov, O.N. Vorobev, S.A. Menshikov, M.S. Ali</i>	
9. A GIS-based assessment of land cover change in an alpine protected area	37
<i>M. Zurlo, B. Bassano, M. Caccianiga</i>	
10. Presence of European beech in its spanish southernmost limit characterized with Landsat intra-annual time series	41
<i>C. Gómez, P. Alejandro, I. Aulló-Maestro, L. Hernández, R. Sánchez de Dios, H. Sainz-Ollero, J.C. Velázquez, F. Montes</i>	
11. Post-hurricane forest mapping in Bory Tucholskie (northern Poland) using random forest-based up-scaling approach of ALS and photogrammetry- based CHM to KOMPSAT-3 and planetscope imagery	45
<i>P. Wężyk, P. Hawryło, K. Zięba-Kulawik</i>	
12. Forest type classification using morphological operators and Forest PA method	49
<i>M. Ustuner, F. B. Sanli, S. Abdikan</i>	
13. Using Google Earth Engine for the analysis of fog and forest landscape interactions in hyper-arid areas of southern Peru	53
<i>E. Forzini, G. Castelli, F. Salbitano, E. Bresci</i>	
14. Detecting tree hedgerows in agroforestry landscapes	57
<i>F. Chiocchini, M. Cioffi, M. Sarti, M. Lauteri, M. Cherubini, L. Leonardi, P. Paris</i>	
15. Evaluating accurate poplar stem profiles by TLS	61
<i>N. Puletti, M. Grotti, R. Scotti</i>	
16. Classification of dominant forest tree species by multi-source very high resolution remote sensing data	65
<i>B. Del Perugia, D. Travaglini, A. Barbati, A. Barzagli, F. Giannetti, B. Lasserre, S. Nocentini, G. Santopuoli, G. Chirici</i>	

17. ALS data for detecting habitat trees in a multi-layered mediterranean forest	69
<i>G. Santopuoli, M. Di Febbraro, C. Alvites, M. Balsi, M. Marchetti, B. Lasserre</i>	
18. Creating a map of reforestation on abandoned agricultural lands in Mari El republic using satellite images	73
<i>S. A. Lezhnin, R. L. Muzurova</i>	
19. Monitoring the growth dynamics of water hyacinth (<i>Eichhornia crassipes</i>)	77
<i>J.F. Mas</i>	
20. Long-term comparison of in situ and remotely-sensed leaf area index in temperate and mediterranean broadleaved forests	81
<i>C. Tattoni, F. Chianucci, M. Grotti, R. Zorer, A. Cutini, D. Rocchini</i>	
21. Evaluation of the atmospheric upward thermal emission towards SSS retrieval at L Band	85
<i>A.V. Bosisio, G. Macelloni, M. Brogioni</i>	
22. Use of Sentinel-1 and Sentinel-3 data to initialize a numerical weather model	88
<i>L. Pulvirenti, M. Lagasio, A. Parodi, G. Venuti, E. Realini, N. Pierdicca</i>	

Earth observation for disaster risk and geomorphologic application93

23. Modelling soil erosion in the Alps with dynamic RUSLE-LIKE MODEL and satellite observations	94
<i>M. Aiello, M. Gianinetto, R. Vezzoli, F. Rota Nodari, F. Polinelli, F. Frassy, M.C. Rulli, G. Ravazzani, C. Corbari, A. Soncini, D.D. Chiarelli, C. Passera, D. Bocchiola</i>	
24. Soil degradation mapping using GIS, remote sensing and laboratory analysis in the Oum Er Rbia high basin, middle atlas, Morocco	98
<i>A.El Jazouli, A. Barakat, R. Khellouk, J. Rais</i>	
25. UAV application for monitoring the annual geomorphic evolution of a coastal dune in Punta Marina (Italy)	103
<i>E. Grottoli, P. Ciavola, E. Duo, A. Ninfo</i>	
26. Thermographic characterization of a landfill trough an Unmanned Aerial Vehicle	108
<i>F. Capodici, G. Dardanelli, M. Lo Brutto, A. Maltese</i>	
27. UAV digital photogrammetric analysis for soil erosion evaluation in the Rivo catchment: preliminary results	114
<i>A. Minervino Amodio, P.P.C. Aucelli, G. Di Paola, V. Garfi, M. Marchetti, C.M. Roskopf, S. Troisi</i>	
28. Exploitation of GNSS for calibrating space-borne SAR for the study of landsubsidence	118
<i>G. Farolfi, M. Del Soldato, S.Bianchini, N. Casagli</i>	
29. Contribution of spatial multi-sensor imagery to the cartography of structural lineaments: case study of the paleozoic massif of Rehamna (moroccan Meseta)	122
<i>I. Serbouti, M. Raji, M. Hakdaoui</i>	

Use of remote sensing for water management and protection126

30. COSMO-SkyMed space data supporting disaster risk reduction	127
<i>F. Lenti, M.L. Battagliere, M. Virelli, A. Coletta</i>	
31. The use of remote sensing for water protection in the karst environment of the tabular middle Atlas/the cause of El Hajeb/Morocco	131
<i>A. Muzirafuti, M. Boualoul, G. Randazzo, S. Lanza, A. Allaoui, H. El Ouardi, H. Habibi, H. Ouhaddach</i>	
32. Analysis of floods, urbanization and morphometry of watersheds in Santo André-Brazil	135
<i>J. Gueiros Fusato, M.C. Valverde</i>	
33. Detection of water bodies using open access satellite data: the case study of Kastoria lake in north-western Greece	139
<i>A. Karagianni</i>	
34. A comparison between UAV and high-resolution multispectral satellite images for bathymetry estimation	143
<i>L. Rossi, I. Mammi, E. Pranzini</i>	
35. Analysis of water bodies under partial cloud conditions using satellite images	147
<i>R. Neware, M. Thakare, U. Shrawankar</i>	
36. Estimating vulnerability of water body using Sentinel-2 images and predictive	

eutrophication models: the study case of Bracciano lake (Italy)	151
<i>C. Giuliani, M. Piccinno, A. Veisz, F. Recanatesi</i>	
Coastal monitoring by remote sensing	156
37. Proneness to future marine inundation of Campania coastal plains (southern Italy) in relation to their subsidence trends assessed by Interferometric SAR techniques	157
<i>G. Di Paola, P.P.C. Aucelli, F. Matano, A. Rizzo</i>	
38. Laser scanner and multibeam integrated survey for the assesment of rocky sea cliff geomorphological hazard	162
<i>S. Guida, N. Corradi, B. Federici, A. Lucarelli, P. Brandolini</i>	
39. Shoreline changes at Sant’Agata river mouth (Reggio Calabria, Italy)	167
<i>G. Barbaro, G. Bombino, V. Fiamma, G. Foti, P. Puntorieri, F. Minniti C. Pezzimenti</i>	
40. Earth observation as an aid to coastal water monitoring: potential application to harmful algal bloom detection	171
<i>C. Lapucci, S. Taddei, B. Doronzo, M. Fattorini, S. Melani, G. Betti, F. Maselli, A. Ortolani, B. Gozzini, C. Brandini</i>	
41. Integrating remote sensing data for the assessments of coastal cliffs hazard: MAREGOT project	176
<i>G. Deiana, M. T. Melis, A. Funedda, S. Da Pelo, M. Meloni, L. Naitza, P. Orrù, R. Salvini, A. Sulis</i>	
42. Coastal monitoring through field and satellite data	181
<i>M.Perna, G. Vitale, C. Brandini, E. Pranzini, B. Gozzini</i>	
Application of remote sensing in urban environments.....	186
43. Remote sensing and urban metrics: an automatic classification of spatial configurations to support urban policies	187
<i>E. Barbierato, I. Bernetti, I. Capecchi, C. Saragosa</i>	
44. Remote sensing of the urban heat island with different spatial and temporal resolutions: analysis by MODIS and LANDSAT imagery	191
<i>S. Bonafoni, C. Keeratikasikorn</i>	
45. Building footprint extraction from VHR satellite imagery using a Deep Learning approach	195
<i>C. Sandu, S. Ghassemi, A. Fiandrotti, F. Giulio Tonolo, P. Boccardo, G. Francini, E. Magli</i>	
46. An integration of VHR OPTICAL and RADAR multiscale images processing data and geographical information system applied to a geo-archeological reconstruction in the Ferrara area	199
<i>L. Damiani, F. Immordino, E. Candigliota</i>	
47. Multitemporal landscape pattern analysis: a quantitative approach to support sustainable land management	203
<i>G. Chirici, P. Rossi, D. Fanfani, D. Poli, M. Rossi, B. Mariolle</i>	

EXPLOITATION OF GNSS FOR CALIBRATING SPACE-BORNE SAR FOR THE STUDY OF LANDSUBSIDENCE

G. Farolfi^{1,2*}, M. Del Soldato¹, S. Bianchini¹, N. Casagli¹

¹ Earth Science Department, University of Firenze, Firenze, Italy –
(gregorio.farolfi, matteo.delsoldato, silvia.bianchini, nicola.casagli)@unifi.it

² Department of Geo-information, Italian Military Geographic Institute, Firenze, Italy

KEY WORDS: GNSS; SAR; Persistent Scatterers Interferometry; deformation map; Calibration, InSAR

ABSTRACT:

Nowadays advanced multi-temporal interferometric approaches such as PSI (Persistent Scatterers Interferometry) derived from the processing of space-borne SAR (Synthetic Aperture Radar) images represent an effective tool to detect terrain movements and provide millimetric ground measurements over large scenes thanks to their wide-area coverage, non-invasiveness, and high accuracy. Nevertheless, PSI data lack of absolute reference both in time and space, as they are relative estimates measured along the sensors-to-target line of sight and referred to a chosen stable motionless reference point. In this work, a methodology to fix relative InSAR results into conventional geodetic reference systems through calibration with GNSS (Global Navigation Satellite System) data acquired from permanent stations is proposed. In particular, mean yearly velocities of PSI radar benchmarks are corrected with GNSS values by means of procedures commonly used in geodesy for combining crustal and local deformation studies. The operative method is tested in the area of Ravenna and Ferrara cities on the north-western Adriatic coast within the eastern alluvial plain of Po River, extensively affected by subsidence with strong spatial and temporal variations. The outcomes reveal the usefulness of the presented methodology for generating unique ground deformation maps over wide areas using geodesy for aligning PSI data before SAR maps stacking.

1. INTRODUCTION

Land subsidence is commonly defined as sudden sinking or gentle and gradual lowering or sudden sinking of the ground surface (Galloway & Burbey, 2011). Natural or anthropogenic processes, as well as their combination, and endogenic or exogenic phenomena, which refer to geological-related motions and the removal of underground materials, respectively, (Prokopovich, 1979) can be caused subsidence, sometimes with consequences. Subsidence phenomena mainly affect urban and greenhouses or nurseries areas (Tomas et al., 2014; Del Soldato et al., 2018) because of water overexploitation, with serious consequences such as damage to linear infrastructures, e.g., bridges, roads or railways, and building stability issues due to differential settlement (Del Soldato et al., 2016; Tomas et al., 2012). The monitoring of these phenomena plays a key role in the management of natural hazards for mitigating and minimizing the disaster losses and consequences. For land subsidence monitoring, classical techniques such as levelling networks (Teatini et al., 2005) or GNSS/GPS (Global Positioning System) techniques (Béjar-Pizarro et al. 2016) are traditionally used. In the last several decades, the Earth Observation (EO) technique, especially SAR (Synthetic Aperture Radar) remote sensing methods have rapidly grown. These techniques can profitably support risk reduction strategies by taking advantage of their wide area coverage associated with a high cost/benefit ratio. The PSI (Persistent Scatterers Interferometry) techniques (e.g. Ferretti et al., 2001 and 2011), has been successfully adopted for a wide range of applications in disaster management, and it has extensively proven to be a valuable tool to detect ground deformations due to landslides (Solari et al., 2018; Del Soldato et al., 2018a; Ciampalini et al., 2016) or subsidence (Bonì et al., 2017; Da Lio & Tosi, 2018a).

PSI is commonly applied to satellite SAR images based on the recognizing on ground points characterized by long-term stability of the electromagnetic backscattered signal and high reflectivity Persistent Scatterers (PS) (Ferretti et al., 2001, Crosetto et al. 2016). By using the interferometric technique on the signal phase reflected by PS, the velocities of these points can be studied through the time-series analysis of their displacements. Such as all the interferometric techniques, the velocity measured are relative to some points of the SAR image that is supposed to be stable. The lack of an absolute reference frame can be supplied by GNSS (Global Navigation Satellite System) measurements (Farolfi et al., 2018, 2019) as this is a geodetic network that provides rates and precise geographic location. In literature, many works exploited both SAR and GNSS data (i.e. Bovenga et al., 2012; Casu et al., 2006; Del Soldato et al., 2018b) for local terrain movements. In this work, we exploit SAR data acquired by historical ENVISAT data supported and calibrated by means of GNSS data throughout a methodological procedure for combining the two source datasets. We apply this approach to Ravenna and Ferrara cities located in the Po Plain in Central Italy, as this area is historically affected by subsidence due to natural and anthropogenic causes (Carminati and Martinelli, 2002). The merging of SAR products with GNSS reveals to be fundamental especially in the case of land subsidence where the velocity rates play an important role to understand and quantify the phenomena.

1. AREA OF STUDY

The paper focuses on the eastern portion of the Po River plain, a narrow area of Italian peninsula between Northern Apennines, Southern Alps and along the northern Adriatic coast where Ravenna and Ferrara cities are located. The Po River sedimentary basin is filled by Alpine and Apennine sediments. From the structural point of view, the north-verging Apennine fold-and-

* Corresponding author

thrust belt system is overlapped by Plio–Quaternary sediments (Carminati, 2002). In this area, vertical deformation is known and the subsidence is driven by the combination of anthropogenic, geological and tectonic processes. The main factor responsible for land subsidence in the Po plain is the human extraction of deep no-rechargeable ground waters (Gambolati et al., 1999). The industrial growth, the modern extensive agricultural and zootechnical techniques and the population increase that took place in the second half of the 20th century in Italy induced a dramatic intensification in groundwater demand. Some authors state that these factors produced a near quadrupling of groundwater withdrawal compared with the first half of the century (Gonella et al., 1998). In addition to water pumping, gas exploitation is also greatly performed in this area during the last century (Teatini et al. 2005, Tosi et al. 2010). Regarding the components of natural subsidence in the Po Plain, the ground lowering is also sediment loading and compaction (Sclater and Christie, 1980) as well as post-glacial rebound and tectonic loading. Geologically, Holocene sediments include sandy and clayey silty level often rich in organic matter and they can suffer from compaction problems by loads and in case of water over-pumping (Rizzetto et al., 2003). Moreover, the effects of the last deglaciation, still impacting the Po Plain (Mitrovica and Davis, 1995), and active tectonics linked to a buried anticline under the Ferrara area are considered additional factors to the long-term geological subsidence (Carminati et al. 2003).

2. DATASETS

2.1 GNSS Dataset

The velocity field for the eastern Po Plain area was derived by the combination of two independent solutions (Palano 2014, Farolfi et al., 2016, 2017) consists of a subset of 35 sites determined for a period that runs from 2008 to 2014. The two velocity solutions were combined involving a rigid Helmert transformation that minimizes the differences of GNSS site velocities that the two datasets have in common, by using a least squares approach. The resulting horizontal velocity field were referred into the European Terrestrial Reference Frame ETRF2008.

2.2 PS dataset

The velocity field determined with SAR satellites were calculated by involving with using PSInSAR technique (Ferretti et al., 2001) by using all available ENVISAT data from the Italian peninsula resulting from the program “Not-Ordinary Plan of Remote Sensing” developed by the Italian Ministry of the Environment available from the Italian Geoportale Nazionale (www.pcn.minambiente.it). The European ENVISAT mission covered a long-term continuous period from 2003 to 2010 with a temporal solution or satellite’s repeating cycle of 35 days.

3. METHODOLOGY

The PS displacements and velocities calculated with GNSS and SAR show differences due to the different LOS direction in which they are recorded. Since the deformation PS velocity is acquired a LOS of the satellites with determined parameters, it must be re-projected and decomposed in vertical and horizontal components to be compared with the velocity components derived by GNSS. For this reason, the LOS displacements and velocities of the ENVISAT PS data was decomposed into horizontal and normal components with respect to the international ellipsoid. After this procedure, the InSAR displacements and velocities can be compared to GNSS dataset.

The velocity v_{LOS} measured by the SAR satellite for a ground velocity v with components $v = [v_N, v_E, v_V]$ is determined by the direction cosine or unit vector $S = [S_N, S_E, S_V]$ in the direction from the ground to the satellite along the LOS direction:

$$v_{LOS} = V_N S_{N,LOS} + V_E S_{E,LOS} + V_V S_{V,LOS} . \quad (1)$$

The unit vector S for ascending (S_A) and descending (S_D) orbits are derived by the inclination of the orbits with respect to the equator $\delta = 98.5^\circ$, and the mean off-nadir θ :

$$\begin{pmatrix} S_A \\ S_D \end{pmatrix} = \begin{pmatrix} -\sin \theta_A \cos \delta & -\sin \theta_A \sin \delta & \cos \theta_A \\ \sin \theta_D \cos \delta & \sin \theta_D \sin \delta & \cos \theta_D \end{pmatrix} \quad (2)$$

For ENVISAT mission the LOS angles for both ascending and descending geometry is given the same value of $\theta = 23.3^\circ$ Eq. 1 can be written for the ascending (V_A) and descending (V_D) velocities with the direction cosine:

$$\begin{pmatrix} V_A \\ V_D \end{pmatrix} = \begin{pmatrix} S_{N,A} & S_{E,A} & S_{V,A} \\ S_{N,D} & S_{E,D} & S_{V,D} \end{pmatrix} \begin{pmatrix} V_N \\ V_E \\ V_V \end{pmatrix} \quad (3)$$

Eq. 3 is a system of two equations with three variables and is thus not solvable. Considering that the displacements along the north–south direction are almost parallel to the ENVISAT satellite orbit and for this reason cannot be detected along the LOS for both the ascending and descending orbits, then eq. 3 can be approximated as:

$$\begin{pmatrix} V_A \\ V_D \end{pmatrix} \cong \begin{pmatrix} S_{E,A} & S_{V,A} \\ S_{E,D} & S_{V,D} \end{pmatrix} \begin{pmatrix} V_E \\ V_V \end{pmatrix} \quad (4)$$

and be solved. The two components of velocity v can be derived as follows:

$$V_E \cong \frac{V_D - V_A}{2 \cdot |S_E|}, \quad V_V \cong \frac{V_D + V_A}{2 \cdot |S_V|} \quad (6)$$

where the modules of unit vectors of S for ENVISAT are $S = [S_N, S_E, S_V] = [0.05, 0.38, 0.92]$. The availability of GNSS site velocity in the Area of Interest (AoI) permits to align the PS velocities to the ETRS89 reference frame. In fact, PS velocities are calculated respect to one or more reference points chosen during the processing phase of the SAR images.

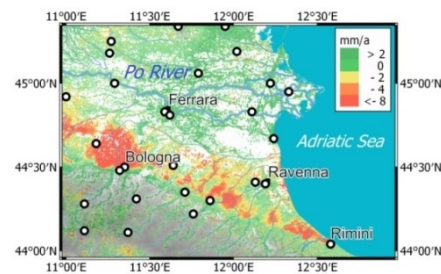


Figure 1 - Map of PS vertical velocity from InSAR images.

Green represents represents stable points, yellow represents points with mild downward movement around -2mm/a , and red represents points of downward movement lower than -8.0 mm/a . Black circles represent the position of GNSS sites.

The lack of an absolute reference frame of PS dataset can be supplied by the comparison of ground point velocities determined using both techniques (Fig.2). The differences between the two velocity datasets were interpolated with an exponential inverse distance weighting to determine the map of correction for PS velocities (Fig.3).

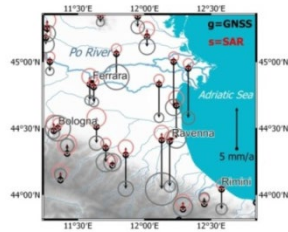


Figure 2 - Comparison of vertical velocities and their circles of uncertainties determinate with GNSS (black arrows) and PSInSAR (red arrows) for each GNSS site (black circles).

4. RESULTS

The GNSS stations displaced in the Po River Delta and in the city of Ravenna record important values lower than -5 mm/a of subsidence. The limit of this lowering ~ -2 mm/a is close to Ferrara. The GNSS stations present in Bologna are stable since they are located out from the wide subsidence area. Rimini show mild values of subsidence ~ -2 mm/y. The comparison between the PS and GNSS vertical velocity shows different rates (Fig. 2) that reach -5 mm/a in the area of Po River Delta and Ravenna, -2 mm/a around Ferrara and Rimini.

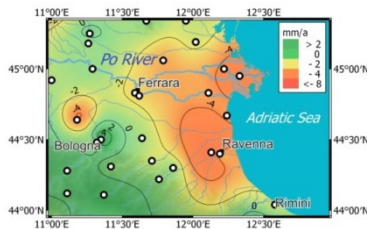


Figure 3 - Calibration map for PS vertical velocity to apply to PS to obtain "absolute" and corrected vertical velocity rates.

The area of the Po River Delta shows subsidence rate with values ~ -5 mm/y (Figure 4). The coastal area from the north of Ravenna town to the city of Rimini shows a bend of subsidence with values variable from -8 mm/a to -4 mm/a confined by stable sector. In the western area of Bologna, is located a big bowl with subsidence rates lower than -10 mm/a. The area of Ferrara town and its surrounding show values of velocity of displacement into the stable span (~ 2 mm/a).

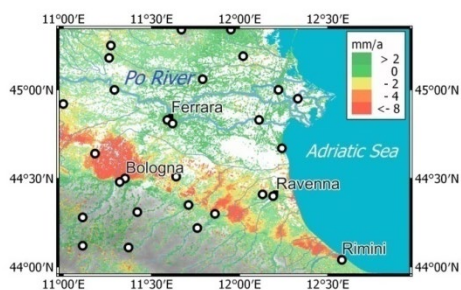


Figure 4 - Vertical velocities of PSI points after the calibration performed by GNSS (absolute velocity). Green represents points with a stable or light uplift, yellow represent points with a mild downward movement, orange represent points with downward movement less than -4 mm/a and red represents points of downward movement less than -8.0 mm/a.

5. CONCLUSIONS

The combination of the GNSS with the PS data deeply improved the investigation of the displacement of the ground. In this way, all the problem of the choice of a stable points for PS processing based on geological and signal features, can be an overpass. The determination of correct vertical velocity rates play an important role in subsiding areas for avoiding damage to structures and infrastructure (e.g. Bianchini et al., 2015; Del Soldato et al., 2016). Moreover, the combination of GNSS and SAR produces new maps of surface movements where velocities at both a detailed and a wider scale are geodetically correct.

CONTRIBUTIONS

Intellectual content to conception and project coordination are contributions of G. Farolfi and N. Casagli. G. Farolfi developed mathematical models and performed the geodetic analysis. S. Bianchini and M. Del Soldato provide SAR analysis, geological settings, geodynamic analysis and the writing of the manuscript. Drafting the article came from the contribution of all the authors. This work received the support of the Department of Earth Sciences, University of Firenze and Istituto Geografico Militare Italiano (IGM). We thank EPN, ASI, INGV and all public and private agencies who run and maintain GNSS networks that publicly share the data. We thank the Ministry of Environment for the SAR datasets used in this study.

REFERENCES

- Bianchini, S., Moretti, S. Analysis of recent ground subsidence in the Sibari plain (Italy) by means of satellite SAR interferometry-based methods. *International Journal of Remote Sensing*, 2015, 36.18: 4550-4569.
- Béjar-Pizarro, M., Guardiola-Albert, C., García-Cárdenas, R.P., Herrera, G., Barra, A., López Molina, A., Tessitore, S., Staller, A., Ortega-Becerril, J.A., Garcia-García, R.P. Interpolation of GPS and geological data using InSAR deformation maps: Method and application to land subsidence in the Alto Guadalentín aquifer (se Spain). *Remote Sens.* 2016, 8, 965.
- Boni, R., Meisina, C., Cigna, F., Herrera, G., Notti, D., Bricker, S., McCormack, H., Tomás, R., Béjar-Pizarro, M., Mulas, J. Exploitation of satellite a-DInSAR time series for detection, characterization and modelling of landsubidence. *Geosciences* 2017.
- Bovenga, F., Wasowski, J., Nitti, D.O., Nutricato, R., T. Chiaradia, M. Using COSMO/SkyMed X-band and ENVISAT C-band SAR interferometry for landslides analysis. *Remote Sensing of Environment* 119 (2012): 272-285.
- Carminati, E., and G. Martinelli. Subsidence rates in the Po Plain, northern Italy: the relative impact of natural and anthropogenic causation. *Engineering Geology* 66.3-4, 2002: 241-255.
- Carminati, E., G. Martinelli, and P. Severi. "Influence of glacial cycles and tectonics on natural subsidence in the Po Plain (Northern Italy): Insights from 14C ages." *Geochemistry, Geophysics, Geosystems* 4.10 (2003).
- Casu, F., M. Manzo, and R. Lanari. "A quantitative assessment of the SBAS algorithm performance for surface deformation retrieval from DInSAR data." *Remote Sensing of Environment* 102.3-4 (2006): 195-210.
- Ciampalini, A., Raspini, F., Frodella, W., Bardi, F., Bianchini, S., Moretti, S. The effectiveness of high-resolution lidar data

- combined with PSInSAR data in landslide study. *Landslides* 2016, 13, 399–410.
- Crosetto, M., Monserrat, O., Cuevas-González, M., Devanthery, N., and Crippa, B. 2016, Persistent Scatterer Interferometry: A review. *International Journal of Photogrammetry and Remote Sensing*, 115, 78–89.
- Da Lio, C., Tosi, L. Land subsidence in the Friuli Venezia Giulia coastal plain, Italy: 1992–2010 results from sar-based interferometry. *Sci. Total Environ.* 2018, 633, 752–764.
- Da Lio, C., Teatini, P., Strozzi, T., Tosi, L. Understanding land subsidence in salt marshes of the Venice lagoon from SAR interferometry and ground-based investigations. *Remote Sens. Environ.* 2018, 205, 56–70.
- Del Soldato, M., Tomás, R., Pont Castillo, J., Herrera García, G., Lopez-Davalillos, G., Carlos, J., & Mora, O. (2016). A multi-sensor approach for monitoring a road bridge in the Valencia harbor (SE Spain) by SAR Interferometry (InSAR).
- Del Soldato, M., Riquelme, A., Bianchini, S., Tomás, R., Di Martire, D., De Vita, P., Moretti, S., Calcaterra, D. Multisource data integration to investigate one century of evolution for the Agnone landslide (Molise, Southern Italy). *Landslides* 2018.
- Del Soldato, M., Farolfi, G., Rosi, A., Raspini, F., Casagli, N. Subsidence Evolution of the Firenze–Prato–Pistoia Plain (Central Italy) Combining PSI and GNSS Data. *Remote Sens.* 2018, 10, 1146.
- Farolfi, G., Del Ventisette, C. 2016, Contemporary crustal velocity field in Alpine Mediterranean area of Italy from new geodetic data. *GPS Solutions*, 204, pp.715-722. ISSN Print 1080-537, doi: 10.1007/s10291-015-0481-1.
- Farolfi, G., Del Ventisette, C. Monitoring the Earth's ground surface movements using satellite observations: Geodynamics of the Italian peninsula determined by using GNSS networks. In *Metrology for Aerospace (MetroAeroSpace)*, 2016 IEEE (pp. 479-483). IEEE.
- Farolfi, G. and Del Ventisette, C. 2017, Strain rates in the Alpine Mediterranean region: insights from advanced techniques of data processing. *GPS Solutions*, 21(3), pp.1027-1036, doi:10.1007/s10291-016-0588-z.
- Farolfi, G., Bianchini, S., Casagli, N. 2018 Integration of GNSS and satellite InSAR data: derivation of fine-scale vertical surface motion maps of Po Plain, Northern Apennines and Southern Alps, Italy, *IEEE Transactions on Geoscience and Remote Sensing (TGRS)*, doi: 10.1109/TGRS.2018.2854371.
- Farolfi, G., Piombino, A., Catani, F. 2019 Fusion of GNSS and satellite radar interferometry: determination of 3D fine-scale map of present-day surface displacements in Italy as expressions of geodynamics processes, *Remote Sensing*.
- Ferretti, A., Prati, C. and Rocca, F. 2001, Permanent Scatterers in SAR Interferometry. *IEEE Trans. On Geosci. Remote Sens.*, 39, p. 8-20.
- Galloway, Devin L., and Thomas J. Burbey. Regional land subsidence accompanying groundwater extraction. *Hydrogeology Journal* 19.8, 2011: 1459-1486.
- Gambolati, G., Teatini, P., Tomasi, L., Gonella, M. Coastline regression of the Romagna region, Italy, due to natural and anthropogenic land subsidence and sea level rise. *Water Resources Research* 35.1 (1999): 163-184.
- Gonella, M., Gambolati, G., Giunta, G., Putti, M., Teatini, P. Prediction of land subsidence due to groundwater withdrawal along the Emilia-Romagna coast. *CENAS*. Springer, Dordrecht, 1998. 151-168.
- GeoportaleNazionale. www.pcn.minambiente.it (20 august 2018).
- Mitrovica, Jerry X., and James L. Davis. Present-day post-glacial sea level change far from the Late Pleistocene ice sheets: Implications for recent analyses of tide gauge records. *Geophysical Research Letters* 22.18 (1995): 2529-2532.
- Palano, M. 2014, On the present-day crustal stress, strain-rate fields and mantle anisotropy pattern of Italy. *Geophysical Journal International*, 200(2), 969-985.
- Prokopovich, Nikola P. Genetic classification of land subsidence. *Evaluation and Prediction of Subsidence*. ASCE, 1979.
- Slater, John G., and Phillip AF Christie. Continental stretching: An explanation of the post-mid-Cretaceous subsidence of the central North Sea basin. *Journal of Geophysical Research: Solid Earth* 85.B7 (1980): 3711-3739.
- Solari, L., Raspini, F., Del Soldato, M., Bianchini, S., Ciampalini, A., Ferrigno, F., Tucci, S., Casagli, N. Satellite radar data for back-analyzing a landslide event: The ponzano (central Italy) case study. *Landslides* 2018, 15, 1–10.
- Teatini, P., Ferronato, M., Gambolati, G., Bretoni, W., Gonella, M., Morelli, M., Severi, P. 2005 Land subsidence due to groundwater withdrawal in the Emilia-Romagna coastland, Italy. In *Land Subsidence. Proceedings of the Seventh International Symposium on Land Subsidence*, Vol. I.
- Teatini, P. Tosi, L., Strozzi, T., Carbognin, L., Wegmüller, U., Rizzetto, F. Mapping regional land displacements in the Venice coastland by an integrated monitoring system. *Remote Sens. Environ.* 2005, 98, 403–413.
- Tomás, R., García-Barba, J., Cano, M., P Sanabria, M., Ivorra, S., Duro, J., Herrera, G.. Subsidence damage assessment of a gothic church using Differential Interferometry and field data. *Structural Health Monitoring* 11.6,2012, 751-762.
- Tomás, Roberto, Romero, R., Mulas, J., Marturià, J.J., Mallorquí, J.J., Lopez-Sanchez, J.M, Herrera, G., Gutiérrez, F., González, P.J., Fernández, J., Duque S., Concha-Dimas, A., Cocksley, G., Castañeda, C., Carrasco, D., Blanco, P. Radar interferometry techniques for the study of ground subsidence phenomena: a review of practical issues through cases in Spain. *Environmental earth sciences* 71.1 (2014): 163-181.
- Tosi, L., Teatini, P., Strozzi, T., Carbognin, L., Brancolini, G., and Rizzetto, F. 2010, Ground surface dynamics in the northern Adriatic coastland over the last two decades. *Rend. Fis. Acc. Lincei.*, 21; S115–S129.



This work is licensed under a Creative Commons Attribution-NonCommercial 4.0 International License.